International Journal of Information, Control and Computer Sciences
ISSN: 2517-9942
Vol:1, No:6, 2007

Semi-Blind Two-Dimensional Code Acquisition in CDMA Communications

Rui Wu and Tapani Ristaniemi

Abstract**—** In this paper, we propose a new algorithm for joint time-delay and direction-of-arrival (DOA) estimation, here called two-dimensional code acquisition, in an asynchronous direct-sequence code-division multiple-access (DS-CDMA) array system. This algorithm depends on eigenvector-eigenvalue decomposition of sample correlation matrix, and requires to know desired user's training sequence. The performance of the algorithm is analyzed both analytically and numerically in uncorrelated and coherent multipath environment. Numerical examples show that the algorithm is robust with unknown number of coherent signals.

Keywords**—** Two-Dimensional Code Acquisition; EV-t; DS-CDMA

I. Introduction

IN DS-CDMA communication systems, the users are distinguished by a user-specific spreading code and they share the same frequency band. Hence the input to receiver is a linear superposition of signals transmitted by all the users via a channel which is characterized mainly by channel fading, multipaths, unknown carrier phase, Doppler offset and additive noise. A prerequisite task for the receiver is to estimate the set of unknown parameters. It is well-known, that the parameter of greatest interest in DS-CDMA system is the time-delay, since after that the estimation of other remaining parameters is easier. When antenna arrays are considered, the direction-of-arrival (DOA) estimation of the signals stands out as another major task. Therefore, two-dimensional code acquisition is required. For two-dimensional code acquisition, the conventional matched filter (MF) [1], maximum likelihood (ML) estimator [2], [3], and subspace based estimators [4]-[9] have been proposed. However, conventional estimator is not resistant to multiple-access-interference (MAI). Moreover, the ML estimator is not received considerable attention due to its resolution and relative computational complexity compared to suboptimal subspace based estimators.

Typically, the subspace based estimators are used for DOA estimation, e.g. multiple signal classification (MUSIC) [10], estimation of signal parameters via rotational invariance techniques (ESPRIT) [11], minimum norm (Min-Norm) [12], method of direction estimation (MODE) [13], weight subspace fitting (WSF) [14]-[16], eigenvector (EV) estimator [17], to name a few. A crucial problem existing in subspace based estimators for DOA estimation is the condition which guarantees a unique solution. In general, the subspace based estimators need the sample correlation matrix to be eigen-decomposed and divided into the signal and noise subspaces, whose orthogonality can be exploited. If received signals are uncorrelated and the noise among antenna elements is spatially white, a unique solution is guaranteed to exist. However, a severe performance degradation of subspace based methods can be caused in highly correlated and coherent multipath channel. In this case, the orthogonality does no longer hold due to rank deficiency of source covariance matrix.

The subspace-based estimators, WSF [14] and MODE [13], were proposed to combat the deleterious effect due to coherency. They are statistically efficient estimators demanding sufficient large Signal-to-Noise (SNR) or large received set of samples (symbols). However, both estimators still require a priori knowledge about the number of coherent signals, which is, naturally, an unknown variable. Spatial smoothing [18] and forward and backward spatial smoothing [19] have also been proposed to deal with coherency problem. However, they require a large number of antenna elements which limit their applicability.

In this paper, we propose a new algorithm for two-dimensional code acquisition which relaxed the aforementioned need for large number of antenna sensors and prior knowledge of coherent signals. The algorithm bases on eigenvector-eigenvalue decomposition of sample correlation matrix, and lends on desired user's training sequence support. Hence, we name it EV-t.

The organization of this paper is as following. In section 2, the system model is presented. In section 3A, EV-t algorithm is introduced. Furthermore, the performance of EV-t algorithm for two-dimensional code acquisition is analyzed in uncorrelated and coherent multipath propagation environments in section 3B. In section 4, a discussion of simulation results is given. In section 5, we draw the main conclusions.

II. System Model

The signal model under consideration is an asynchronous multiuser DS-CDMA model with a fading multipath channel. The baseband signal of kth user is formed

$$x_k(t) = \sum_{i=1}^{I} b_{k,i} s_k(t - iT) \tag{1}$$

where $b_{k,i} \in \{-1, 1\}$ is the kth user's data symbol. T denote one symbol duration. The spreading code assigned to kth user is modelled as $s_k(t) = \sum_{n=1}^{N} s_{k,n} \Pi(t - nT_c)$, where $s_{k,n} \in$

Manuscript received February 6, 2006. This work is supported in part by the Academy of Finland.

Rui Wu is with the Department of Mathematical Information Technology, University of Jyväskylä, P.O.Box 35 (Agora), FIN-40014, University of Jyväskylä, Finland (e-mail: ruiwu@cc.jyu.fi).

Tapani Ristaniemi is with the Institute of Communications Engineering, Tampere University of Technology, P.O.Box 553, FIN-33101 Tampere, Finland (e-mail: tapani.ristaniemi@tut.fi).

$\{-1,+1\}$, $\Pi(t)$ denotes a unit rectangular pulse over the chip period T_c which is zero outside of $0 \le t \le T_c$. $N = T/T_c$ is the processing gain.

Without loss of generality, we assume for simplicity that the receiver is equipped with an M-element uniform linear array. We make a standard narrowband assumption where the signal bandwidth is much smaller than carrier frequency. This implies that the time delay due to physical array only cause a phase shift on the impinging signals. Hence, the received signal at the mth antenna sensor can be expressed as

$$\begin{aligned} r^m(t) &= \sum_{k=1}^{K}\sum_{l=1}^{L} b_{k,i}a_{k,l,i}s_k(t-iT-\tau_{k,l}) \\ &\quad e^{j(m-1)\pi\sin(\theta_{k,l})} + n^m(t) \end{aligned} \tag{2}$$

where the fading coefficient $a_{k,l,i}$ may vary from symbol to symbol. Variables $\tau_{k,l}$ and $\theta_{k,l}$ are time delay and direction-of-arrival (DOA), respectively. They are assumed to remain roughly constant within the observation interval.

Assuming that the front-end of each antenna sensor is equipped with a chip-MF to convert a continuous-time signal to discrete-time signal, the sampled output of $r^m(t)$ may be written as

$$r^m[n] = \frac{1}{T_c}\int_{iT_c}^{(i+1)T_c} r^m(t)dt \tag{3}$$

Because of asynchronous transmission, the time reference is arbitrarily aligned to the transmitted bit boundaries. For getting one whole transmitted bit within the window, the observation window can be enlarged into the size of two symbols. Thus, $\mathbf{r}^m(t) \in \mathbb{C}^{2N}$ at time i is

$$\mathbf{r}_i^m = [r^m[iN+1], r^m[iN+2], ..., r^m[(i+2)N]] \tag{4}$$

Therefore, the sampled signal at mth sensor for ith symbol is described by

$$\begin{aligned} \mathbf{r}_i^m &= \sum_{k=1}^{K}\sum_{l=1}^{L}[b_{k,i-1}a_{k,l,i-1}\underline{\mathbf{c}}_{k,l}e^{j(m-1)\pi\sin(\theta_{k,l})} \\ &+ b_{k,i}a_{k,l,i}\mathbf{c}_{k,l}e^{j(m-1)\pi\sin(\theta_{k,l})} \\ &+ b_{k,i+1}a_{k,l,i+1}\overline{\mathbf{c}}_{k,l}e^{j(m-1)\pi\sin(\theta_{k,l})}] + \mathbf{n}_i^m \end{aligned} \tag{5}$$

where

$$\begin{aligned} \underline{\mathbf{c}}_{k,l} &= \underline{\mathbf{c}}_{k,l}(\tau_{k,l}) = (1-\zeta_{k,l})\underline{\mathbf{g}}_{k,l}(h_{k,l}) + \zeta_{k,l}\underline{\mathbf{g}}_{k,l}(h_{k,l}+1) \\ \mathbf{c}_{k,l} &= \mathbf{c}_{k,l}(\tau_{k,l}) = (1-\zeta_{k,l})\mathbf{g}_{k,l}(h_{k,l}) + \zeta_{k,l}\mathbf{g}_{k,l}(h_{k,l}+1) \\ \overline{\mathbf{c}}_{k,l} &= \overline{\mathbf{c}}_{k,l}(\tau_{k,l}) = (1-\zeta_{k,l})\overline{\mathbf{g}}_{k,l}(h_{k,l}) + \zeta_{k,l}\overline{\mathbf{g}}_{k,l}(h_{k,l}+1) \end{aligned}$$

The "previous", "current", and the "next" code vectors can be written, respectively, as

$$\begin{aligned} \underline{\mathbf{g}}_{k,l} &= \underline{\mathbf{g}}_{k,l}(h_{k,l}) = [s_{k,N-h_{k,l+1}}, ..., s_{k,N}, \overbrace{0,\ldots,0}^{2N-h_{k,l}}]^T \\ \mathbf{g}_{k,l} &= \mathbf{g}_{k,l}(h_{k,l}) = [0,\ldots,0,s_{k,1},\ldots,s_{k,N},0,\ldots,0]^T \\ \overline{\mathbf{g}}_{k,l} &= \overline{\mathbf{g}}_{k,l}(h_{k,l}) = [\underbrace{0,\ldots,0}_{N+h_{k,l}}, s_{k,1},\ldots,s_{k,N-h_{k,l}}]^T \end{aligned}$$

The exact time delay of kth user's lth path can be expressed as $\tau_{k,l} = h_{k,l}T_c + \zeta_{k,l}$, where $h_{k,l}$ and $\zeta_{k,l}$ are the integer and fractional part of time delay $\tau_{k,l}$, respectively.

The overall sampled signal at the antenna array sensors is expressed as

$$\begin{aligned} \mathbf{r}_i &= \sum_{k=1}^{K}\sum_{l=1}^{L}[b_{k,i-1}a_{k,l,i-1}\underline{\mathbf{c}}_{k,l}\otimes\mathbf{a}_{k,l} \\ &+ b_{k,i}a_{k,l,i}\mathbf{c}_{k,l}\otimes\mathbf{a}_{k,l} \\ &+ b_{k,i+1}a_{k,l,i+1}\overline{\mathbf{c}}_{k,l}\otimes\mathbf{a}_{k,l}] + \mathbf{n}_i \end{aligned} \tag{6}$$

where $\mathbf{a}_{k,l} = [1, e^{j\pi\sin(\theta_{k,l})}, \ldots, e^{j(M-1)\pi\sin(\theta_{k,l})}]^T$. Similar to the array response vectors $\mathbf{a}_{k,l}$, the space-time response vectors are defined as

$$\begin{aligned} \underline{\mathbf{h}}_{k,l} &= \underline{\mathbf{h}}_{k,l}(\theta,\tau) = \underline{\mathbf{c}}_{k,l}\otimes\mathbf{a}_{k,l} \\ \mathbf{h}_{k,l} &= \mathbf{h}_{k,l}(\theta,\tau) = \mathbf{c}_{k,l}\otimes\mathbf{a}_{k,l} \\ \overline{\mathbf{h}}_{k,l} &= \overline{\mathbf{h}}_{k,l}(\theta,\tau) = \overline{\mathbf{c}}_{k,l}\otimes\mathbf{a}_{k,l} \end{aligned} \tag{7}$$

where $\otimes$ denotes the Kronecker product of the two vectors. Finally, the compact representation of (6) can be expressed as

$$\mathbf{r}_i = \mathbf{H}\mathbf{A}_i\mathbf{b}_i + \mathbf{n}_i \tag{8}$$

here $2MN \times 3KL$ matrix $\mathbf{H} = [\underline{\mathbf{h}}_{1,1}, \mathbf{h}_{1,1}, \overline{\mathbf{h}}_{1,1}, ..., \underline{\mathbf{h}}_{K,L}, \mathbf{h}_{K,L}, \overline{\mathbf{h}}_{K,L}]$. The dimension of $\mathbf{A}_i$ corresponding to ith sampled symbol is $3KL \times 3K$. Its expression is $\mathbf{A}_i = diag\{\mathbf{A}_{1,i}, ..., \mathbf{A}_{k,i}, ...\mathbf{A}_{K,i}\}$ and

$$\mathbf{A}_{k,i} = \begin{pmatrix} a_{k,1,i-1} & 0 & 0 \\ 0 & a_{k,1,i} & 0 \\ 0 & 0 & a_{k,1,i+1} \\ \vdots & \vdots & \vdots \\ a_{k,L,i-1} & 0 & 0 \\ 0 & a_{k,L,i} & 0 \\ 0 & 0 & a_{k,L,i+1} \end{pmatrix} \tag{9}$$

$\mathbf{b}_i = [b_{1,i-1}, b_{1,i}, b_{1,i+1}, \ldots, b_{K,i-1}, b_{K,i}, b_{K,i+1}]^T$. Symbols are random and independent binary variables with zero mean, e.g. $E\{b_{k,i}\} = 0$, and $E\{b_{k,i}b_{p,j}\} = 0$ if $k \ne p$ and/or $i \ne j$. Symbols are also uncorrelated with fading coefficients. $\mathbf{n}_i$ is $3K \times 1$ noise vector. The noise is independent zero mean circular complex Gaussian random variable which are uncorrelated with symbols and fading coefficients.

III. Two-Dimensional Code Acquisition Problem

Subspace based estimator need the eigen-decomposition of ensemble correlation matrix. The ensemble correlation matrix of $\mathbf{r}_i$ can be written as

$$\begin{aligned} \mathbf{R}_r &= E\{\mathbf{r}_i\mathbf{r}_i^H\} \\ &= E\{(\mathbf{H}\mathbf{A}_i\mathbf{b}_i + \mathbf{n}_i)(\mathbf{H}\mathbf{A}_i\mathbf{b}_i + \mathbf{n})_i^H\} \\ &= \mathbf{H}\mathbf{R}_A(i)\mathbf{H}^H + \sigma^2\mathbf{I} \end{aligned} \tag{10}$$

The correlation matrix $\mathbf{R}_A(i) = diag\{\mathbf{R}_A(1,i), ..., \mathbf{R}_A(k,i), ...\mathbf{R}_A(K,i)\}$. $\mathbf{R}_A(k,i)$ is shown at the top of the next page, and $a'_{k,(l,l'),i-1} = E\{a_{k,l,i-1}a^*_{k,l',i-1}\}$, $a'_{k,(l,l'),i} = E\{a_{k,l,i}a^*_{k,l',i}\}$, $a'_{k,(l,l'),i+1} = E\{a_{k,l,i+1}a^*_{k,l',i+1}\}$. The ensemble correlation matrix $\mathbf{R}_r$ can be eigen-decomposed as

$$\mathbf{R}_r = \sum_{d=1}^{2NM}\lambda_d\mathbf{u}_d\mathbf{u}_d^H \tag{12}$$

$$\mathbf{R}_A(k,i) = \tag{11}$$

$$\begin{pmatrix}
a'_{k,(1,1),i-1} & 0 & 0 & \cdots & a'_{k,(1,L),i-1} & 0 & 0 \\
0 & a'_{k,(1,1),i} & 0 & \cdots & 0 & a'_{k,(1,L),i} & 0 \\
0 & 0 & a'_{k,(1,1),i+1} & \cdots & 0 & 0 & a'_{k,(1,L),i+1} \\
\vdots & \vdots & \vdots & \vdots & \vdots & \vdots & \vdots \\
a'_{k,(L,1),i-1} & 0 & 0 & \cdots & a'_{k,(L,L),i-1} & 0 & 0 \\
0 & a'_{k,(L,1),i} & 0 & \cdots & 0 & a'_{k,(L,L),i} & 0 \\
0 & 0 & a'_{k,(L,1),i+1} & \cdots & 0 & 0 & a'_{k,(L,L),i+1}
\end{pmatrix}$$

where $\lambda_1 \geq \lambda_2 \geq \cdots \geq \lambda_D \geq \lambda_{D+1} = \cdots = \lambda_{2NM} = \sigma^2$ are eigenvalues of $\mathbf{R}_r$ in descending order, and $\mathbf{u}_d$, $d = 1, \cdots, 2MN$, are the corresponding eigenvectors. We refer to the subspace spanned by $\mathbf{u}_1, ..., \mathbf{u}_D$ as signal subspace and $\mathbf{u}_{D+1}, ..., \mathbf{u}_{2MN}$ as noise subspace. The ensemble correlation matrix may be written as

$$\mathbf{R}_r = \mathbf{U}_s \mathbf{\Lambda}_s \mathbf{U}_s^H + \mathbf{U}_n \mathbf{\Lambda}_n \mathbf{U}_n^H \tag{13}$$

Practically, the ensemble correlation matrix $\mathbf{R}_r$ is not available, and a sample correlation matrix $\hat{\mathbf{R}}_r$ is used instead and eigen-decomposed

$$\hat{\mathbf{R}}_r = \frac{1}{I}\sum_{i=1}^{I} \mathbf{r}_i \mathbf{r}_i^H = \hat{\mathbf{U}}_s \hat{\mathbf{\Lambda}}_s \hat{\mathbf{U}}_s^H + \hat{\mathbf{U}}_n \hat{\mathbf{\Lambda}}_n \hat{\mathbf{U}}_n^H \tag{14}$$

A. EV-t Algorithm for Two-Dimensional Code Acquisition

We consider a general cost function for parameter estimation as

$$\{\hat{\tau}_{1,1}, \hat{\theta}_{1,1}, \cdots, \hat{\tau}_{1,L}, \hat{\theta}_{1,L}\} = \hat{\mathbf{h}}_1^H \mathcal{H}(\mathbf{R}) \hat{\mathbf{h}}_1 \tag{15}$$

where $\hat{\mathbf{h}}_1 = \mathbf{c}_1 \otimes \mathbf{a}$ is a replica of the first user's space-time code vector. A natural extension of the general cost function can be with a different definition of $\mathcal{H}(\mathbf{R})$, e.g. $\mathcal{H}(\mathbf{R}) = \hat{\mathbf{U}}_n \hat{\mathbf{U}}_n^H$ results in MUSIC estimator, and $\mathcal{H}(\mathbf{R}) = \hat{\mathbf{U}}_n \hat{\Lambda}_n^{-1} \hat{\mathbf{U}}_n^H$ is eigenvector (EV) estimator. Different with the general subspace based estimators, e.g. MUSIC, EV estimator, the proposed algorithm, called EV-t, looks for a maximum projection of desired signal's space-time direction onto signal subspace with the support of training sequence. In this case, the weight vector of EV-t for two-dimensional code acquisition is defined as

$$\mathbf{w}_{EV-t} = \hat{\mathbf{U}}_s \hat{\mathbf{\Lambda}}_s^{-1} \hat{\mathbf{U}}_s^H \check{\mathbf{h}}_1 \tag{16}$$

Due to the uncorrelatedness of the symbols, $E\{\mathbf{H}\mathbf{A}_i \mathbf{b}_i b_{1,i}\} = \sum_{l=1}^{L} \mathbf{h}_{1,l} a_{1,l,i}$. Hence the first user's training sequence $\mathbf{B}_1 = [b_{1,1}, ..., b_{1,I}]^T$ can be used to roughly estimate $\check{\mathbf{h}}_1$. Since then we have $\check{\mathbf{h}}_1 = \sum_{l=1}^{L} \mathbf{h}_{1,l} a_{1,l} + \check{\mathbf{n}}$, where $a_{1,l} = \sum_{i=1}^{I} a_{1,l,i}$.

The parameters are estimated by searching the maximum peaks through two-dimensional spectra. If eigenvalues/eigenvectors are accurately estimated, L maximum peaks indicating space-time directions of the first user can be catched.

B. Performance Analysis

In this section, we analyze the performance of EV-t estimator. Specifically, we address the limitations of this estimator resulted from the perturbation on the estimated eigenvalue and eigenvectors in the signal subspace, and the estimated $\check{\mathbf{h}}_1$.

In [20], the perturbation of estimated eigenvalues and eigenvector are discussed. In [21], the estimated eigenvalues $\hat{\lambda}_d$, $d = 1, ..., D$, corresponding to the signal subspace are expressed as

$$\hat{\lambda}_d = \lambda_d + \frac{1}{\sqrt{I}} \beta_{d,d} \tag{17}$$

$\beta_{d,d}$ is the dth diagonal component of the hermitian matrix $[\beta_{d,f}]$ with the following statistical properties

$$E[\beta_{d,f}] = 0 \tag{18}$$

$$E[\beta_{d,f} \beta_{e,g}^*] = \mathbf{u}_d^H \mathbf{R}_r \mathbf{u}_e \mathbf{u}_g^H \mathbf{R}_r \mathbf{u}_f = \lambda_d \lambda_f \delta_{d,e} \delta_{f,g} \tag{19}$$

where $\delta_{d,e} = 1$ only if $d = e$, otherwise $\delta_{d,e} = 0$. Meanwhile, the associated eigenvectors $\hat{\mathbf{u}}_d$, $d = 1, ..., D$, are [21]

$$\begin{aligned}
\hat{\mathbf{u}}_d &= [1 - \frac{1}{2I} \sum_{\substack{f=1 \\ f \neq d}}^{2NM} |v_{f,d}|^2] \mathbf{u}_d + \frac{1}{\sqrt{I}} \sum_{\substack{f=1 \\ f \neq d}}^{2NM} v_{f,d} \mathbf{u}_f \\
&- \frac{1}{2I\sqrt{I}} \sum_{\substack{f=1 \\ f \neq d}}^{2NM} \sum_{\substack{i=1 \\ i \neq d}}^{2NM} |v_{f,d}|^2 v_{i,d} \mathbf{u}_i + O(\frac{1}{I^2})
\end{aligned} \tag{20}$$

and

$$v_{f,d} = \begin{cases} \dfrac{\beta_{f,d}}{(\lambda_d - \lambda_f)} & \text{if } d, f = 1, ..., D, d \neq f, \\ \dfrac{\beta_{f,d}}{(\lambda_d - \sigma^2)} & \text{if } d = 1, ..., D, \\ & f = D+1, ..., 2NM. \end{cases} \tag{21}$$

Because $\hat{\lambda}_d^{-1} = \frac{1}{\lambda_d}(1 - \frac{\beta_{d,d}}{(\sqrt{I}\lambda_d + \beta_{d,d})}) \approx \frac{1}{\lambda_d}(1 - \frac{\beta_{d,d}}{\sqrt{I}\lambda_d})$, the mean of $\hat{\mathbf{u}}_d \hat{\lambda}_d^{-1} \hat{\mathbf{u}}_d^H$ (Appendix A) is

$$\begin{aligned}
&E\{\hat{\mathbf{u}}_d \hat{\lambda}_d^{-1} \hat{\mathbf{u}}_d^H\} \\
&= \frac{1}{\lambda_d} \mathbf{u}_d \mathbf{u}_d^H - \frac{1}{I} \sum_{\substack{f=1 \\ f \neq d}}^{2NM} \frac{\lambda_f}{(\lambda_d - \lambda_f)^2} \mathbf{u}_d \mathbf{u}_d^H \\
&+ \frac{1}{I} \sum_{\substack{f=1 \\ f \neq d}}^{2NM} \frac{\lambda_f}{(\lambda_d - \lambda_f)^2} \mathbf{u}_f \mathbf{u}_f^H + O(\frac{1}{I^2})
\end{aligned} \tag{22}$$

1) Performance Analysis for Uncorrelated Multipath Propagation: To clarify and simplify the derivation, a rational assumption that $\mathbf{h}_{1,1}$ happens to match $\mathbf{u}_1$, $\mathbf{h}_{1,2}$ matches $\mathbf{u}_2$ and so on until $\mathbf{h}_{1,L}$ happens to match $\mathbf{u}_L$ is made here. Among L maximum peaks, the performance analysis at below focuses on the first path of the first user. After a series of algebraic manipulations (see appendix B), we get

$$E\{\mathbf{w}_{EV-t}^H\hat{\mathbf{h}}_1\}_{un} = \check{\mathbf{h}}_1^H\sum_{d=1}^{D}E\{\hat{\mathbf{u}}_d\hat{\lambda}_d^{-1}\hat{\mathbf{u}}_d^H\}\hat{\mathbf{h}}_1 \quad (23)$$

$$= a_{1,1}\mathbf{h}_{1,1}^H\mathbf{u}_1\lambda_1^{-1}\mathbf{u}_1^H\hat{\mathbf{h}}_1 + \chi a_{1,1}\mathbf{h}_{1,1}^H\mathbf{u}_1\mathbf{u}_1^H\hat{\mathbf{h}}_1 + O(\frac{1}{I^2})$$

Because of uncorrelated multipath propagation, we define $D = 3KL$. The perturbation coefficient χ is

$$\chi = \frac{1}{I}(\sum_{d=2}^{D}\frac{1}{(\lambda_1-\lambda_d)} - \frac{\sigma^2(2NM-D)}{(\lambda_1-\sigma^2)^2}) \quad (24)$$

2) Performance Analysis for Coherent Multipath Propagation: In this case, the performance analysis bases on the assumption of $\mathbf{h}_{1,1},...,\mathbf{h}_{1,L}$ lying along the same direction of $\mathbf{u}_1$. After a series of algebraic manipulations (see appendix C), the performance of EV-t for the first path of the first user is derived as

$$E\{\mathbf{w}_{EV-t}^H\hat{\mathbf{h}}_1\}_{co} = \check{\mathbf{h}}_1^H\sum_{d=1}^{D}E\{\hat{\mathbf{u}}_d\hat{\lambda}_d^{-1}\hat{\mathbf{u}}_d^H\}\hat{\mathbf{h}}_1 \quad (25)$$

$$= a_{1,1}\mathbf{h}_{1,1}^H\mathbf{u}_1\lambda_1^{-1}\mathbf{u}_1^H\hat{\mathbf{h}}_1 + \chi a_{1,1}\mathbf{h}_{1,1}^H\mathbf{u}_1\mathbf{u}_1^H\hat{\mathbf{h}}_1$$

$$+ \sum_{l=2}^{L}(a_{1,l}\lambda_1^{-1} + \chi_l a_{1,l})\mathbf{h}_{1,l}^H\mathbf{u}_1\mathbf{u}_1^H\hat{\mathbf{h}}_1 + O(\frac{1}{I^2})$$

Compared with (23), an extra error-term $\sum_{l=2}^{L}(a_{1,l}\lambda_1^{-1} + \chi_l a_{1,l})\mathbf{h}_{1,l}^H\mathbf{u}_1\mathbf{u}_1^H\hat{\mathbf{h}}_1$ is in (25). Because of unknown number of coherent signals, we still define $D = 3KL$. The perturbation coefficient χ_l is given as

$$\chi_l = \frac{1}{I}(\sum_{\substack{d=1\\d\neq l}}^{D}\frac{1}{(\lambda_l-\lambda_d)} - \frac{\sigma^2(2NM-D)}{(\lambda_l-\sigma^2)^2}) \quad (26)$$

From (23) and (25) we see that the performance of $E\{\mathbf{w}_{EV-t}^H\hat{\mathbf{h}}_1\}_{un}$ and $E\{\mathbf{w}_{EV-t}^H\hat{\mathbf{h}}_1\}_{co}$ highly depends on the fading coefficients, e.g. $a_{1,1}$ and $a_{1,l}$, and perturbation coefficients, e.g. χ and χ_l. Because $a_{1,l} = \sum_{i=1}^{I}a_{1,l,i}$, its probability distribution can not be defined. A severe performance degradation can be caused by $a_{1,l}$ with increasing length of training sequence I. If noise is small enough, we can see that χ and χ_l are inversely proportional with I and eigenvalue λ_d, and are proportional with dimensionality $2MN-D$. The second parts of χ and χ_l are on the inverse square λ_d, hence the activity of $2MN-D$ has a great decrement with increasing λ_d. λ_d, $d = 1,...,D$, are proportional with signal strengths and the length of space-time response vector (see Appendix D). We note here that I plays a negative role in $a_{1,l}$ and a positive role in χ and χ_l.

IV. Simulation Results

In this section we give some numerical examples to illustrate the observations got from the analysis above. In addition, we compare the results to those of traditional MUSIC in an asynchronous DS-CDMA uplink channel where the received multiuser signals undergo frequency selective Rayleigh fading. The Rayleigh fading processes are conducted as following: the carrier frequency is $f_c = 1.8$GHz, the mobile speed is $v = 50$km/h, and the symbol rate is $1/T = 16$kbit/s. Hence, the maximum Doppler shift is $f_d = (\frac{v}{v_c})f_c = 83.3Hz$, and the channel coherence time T_{coh} is equal to $\frac{1}{f_d} = 0.012s$.

For each simulation, only the code and training sequence of first user are known. Any parameters, such as time-varying Rayleigh fading coefficients, are assumed to be unknown. Gold codes of length $N = 15$ are used for spreading. A uniform linear array with half a wavelength sensor spacing is used. Time delays are assumed discrete and uniformly distributed over $[0, 0.1, ..., 14]$ chips. The angle spread is within a span of 60°. The number of users K is set as 3 and the number of resolvable paths is $L = 2$. Therefore, the total number of source signals is $3KL$, where the maximum signal subspace dimension is defined $D = 3KL$. In case of coherent multipath simulation, we still define $D = 3KL$ due to the unknown number of coherent signals. We assume the first path delay $\tau_{1,1} < \tau_{1,l}$ for $l \neq 1$. SNRs in the chip-MF output is always 10dB. All simulation results are based on 1000 independent runs. The performance measure is defined as the probability of successful acquisition. A successful acquisition is regarded when the estimation error of time delay is less than half a chip, and the estimation error of DOA is less than 3°.

A. Effect of channel correlation

In this experiment, we examine the effect of channel correlation which varies from 0.1 to 1. The system includes $K = 3$ users in an equal-energy two-path Rayleigh fading channel. The average SNR is 10dB and all interfering users are 10dB stronger. The number of antenna sensors is 12, and D is fixed to $3KL$.

Fig. 1 shows the achieved probabilities of acquisition as a function of correlation coefficient. Predictably, MUSIC fails due to the existence of coherent multipaths. However, the acquisition probabilities of EV-t are acceptable and remain almost on the same level regardless of the correlation coefficient.

B. Effect of MAI

Here we study the effect of increasing the level of MAI per interfering user in uncorrelated and coherent multipath environments, respectively. The system includes $K = 3$ users in an equal-energy two-path Rayleigh fading channel. The average SNR is 10dB. The number of antenna sensors is 12 and $D = 3KL$.

Fig. 2 shows the achieved probabilities of acquisition as a function of MAI per interfering user for uncorrelated multipath propagation. In this case, the correlation coefficient between the paths for each user is zero. Fig. 2 shows that the acquisition

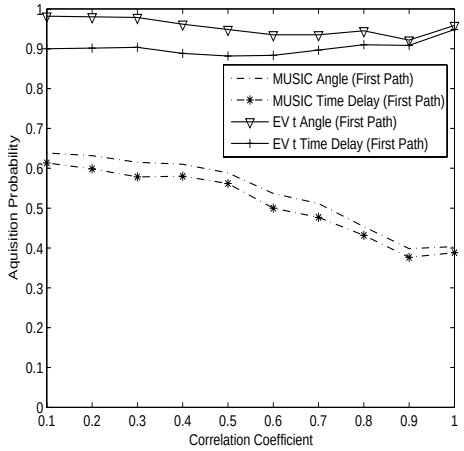

Fig. 1. Probability of acquisition as a function of multi-path correlation coefficient in an equal-energy two-path Rayleigh fading channel. The system includes $K = 3$ users. The length of training sequences is 50. All the interfering users are 10dB stronger. The number of antenna sensors is 12 and the average SNR is 10 dB.

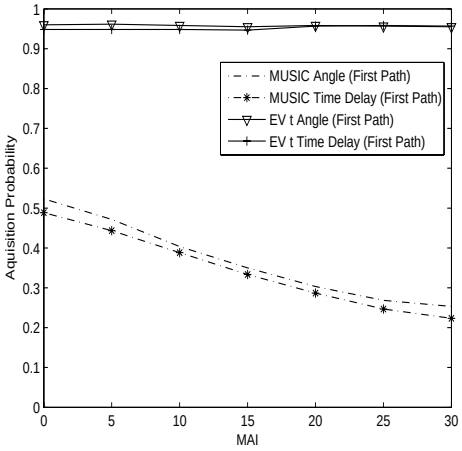

Fig. 3. Probability of acquisition as a function of MAI in an equal-energy two-path Rayleigh fading channel. The system includes $K = 3$ users. The length of the training sequence is 50. The number of antenna sensors is 12, the average SNR is 10dB and the correlation coefficient between the paths is 1.

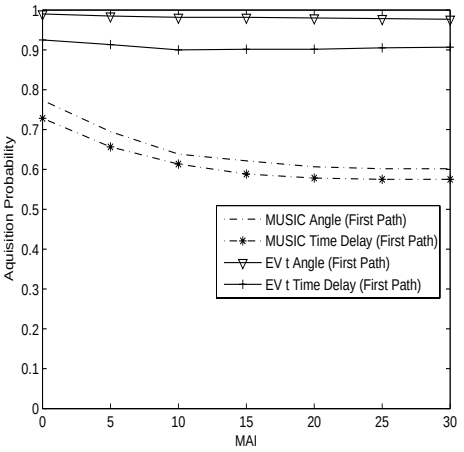

Fig. 2. Probability of acquisition as a function of MAI in an equal-energy two-path Rayleigh fading channel. There are $K = 3$ users is the system. The length of the training sequence is 50. The number of antenna sensors is 12, the average SNR is 10dB and the correlation coefficient between the paths is 0.

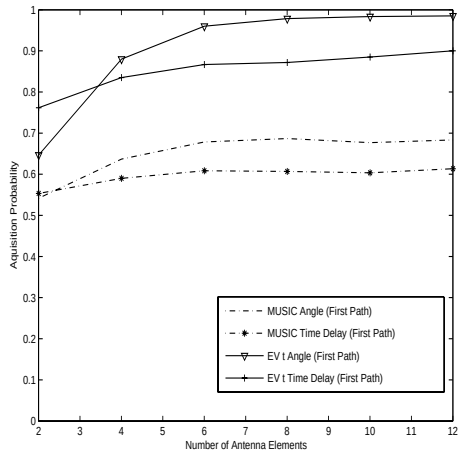

Fig. 4. Acquisition probability as a function of the number of antenna sensors in an equal-energy two-path Rayleigh fading channel. The system includes $K = 3$ users. The length of training sequence is 50. The average SNR is 10dB and all the interfering users are 10dB stronger. Correlation coefficient between the paths is 0.

probabilities of EV-t are invariant, even if MAI reaches to 30dB. However, MUSIC fails in higher MAI scenario. Fig. 3 shows the achieved probabilities of acquisition for coherent multipath propagation. In this simulation, the correlation coefficient between paths of each user is set 1. If noise is small enough, square signal strengths have inversely proportional with $2NM - d$. Hence, one can see that the acquisition probabilities of EV-t in Fig. 3 are still as good as they are in Fig. 2.

C. Effect of the number of antenna sensors

In this set of experiments, we study the effect of number of antenna sensors. The system includes $K = 3$ users in an equal- energy two-path Rayleigh fading channel. The average SNR is 10dB and all the interfering users are 10dB stronger. D is set to $3KL$.

Figs. 4 and 5 show the achieved probabilities of acquisition as function of number of antenna sensors for uncorrelated and coherent multipath scenario, respectively. The two figures show that the performance of MUSIC has not a great improvement with the increasing number of antenna sensors. However, EV-t depends essentially on the length of space-time response vector. It is hence expected that with large number of antenna sensors the performance of EV-t can be greatly improved, as can be seen in Figs. 4 and 5.

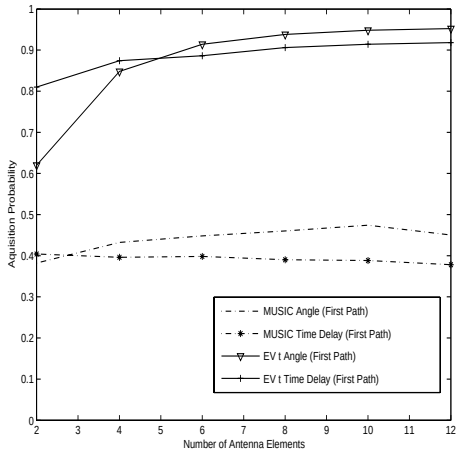

Fig. 5. Acquisition probability as a function of the number of antenna sensors in an equal-energy two-path Rayleigh fading channel. The system includes $K = 3$ users. The length of training sequence is 50. The average SNR is 10dB and all the interfering users are 10dB stronger. Correlation coefficient between the paths is 1.

V. Conclusion

In this paper, we introduced a new algorithm, named EV-t, for the two-dimensional code acquisition problem in DS-CDMA arrays. The algorithm was analytically analyzed and illustrated by numerical examples. It was observed that the main benefit of EV-t is that it is a robust algorithm to perform parameter estimation regardless of the multipath channel correlation.

Appendix A

At first, the mean of $\hat{\mathbf{u}}_d\hat{\lambda}_d^{-1}\hat{\mathbf{u}}_d^H$ is examined. With the assumption of $\beta_{d,d} \ll \lambda_d$, we have $\hat{\lambda}_d^{-1} = \frac{1}{\lambda_d}(1 - \frac{\beta_{d,d}}{(\sqrt{I}\lambda_d+\beta_{d,d})}) \approx \frac{1}{\lambda_d}(1 - \frac{\beta_{d,d}}{\sqrt{I}\lambda_d})$, in this case, $\hat{\mathbf{u}}_d\hat{\lambda}_d^{-1}\hat{\mathbf{u}}_d^H$ can be assumed asymptotically equals to $\frac{1}{\lambda_d}\hat{\mathbf{u}}_d(1 - \frac{\beta_{d,d}}{\sqrt{I}\lambda_d})\hat{\mathbf{u}}_d^H = \frac{1}{\lambda_d}\hat{\mathbf{u}}_d\hat{\mathbf{u}}_d^H - \hat{\mathbf{u}}_d\frac{\beta_{d,d}}{\sqrt{I}\lambda_d^2}\hat{\mathbf{u}}_d^H$. Substituting (20) into $\frac{1}{\lambda_d}\hat{\mathbf{u}}_d\hat{\mathbf{u}}_d^H$ and $\hat{\mathbf{u}}_d\frac{\beta_{d,d}}{\sqrt{I}\lambda_d^2}\hat{\mathbf{u}}_d^H$, we get

$$\begin{aligned}
&\frac{1}{\lambda_d}\hat{\mathbf{u}}_d\hat{\mathbf{u}}_d^H \qquad (27)\\
=\ &\frac{1}{\lambda_d}\mathbf{u}_d\mathbf{u}_d^H - \frac{1}{I\lambda_d}\sum_{\substack{f=1\\f\neq d}}^{2NM}|v_{f,d}|^2\mathbf{u}_d\mathbf{u}_d^H\\
+\ &\frac{1}{\sqrt{I}\lambda_d}[\sum_{\substack{f=1\\f\neq d}}^{2NM}v_{f,d}\mathbf{u}_f\mathbf{u}_d^H + v_{f,d}^*\mathbf{u}_d\mathbf{u}_f^H]\\
+\ &\frac{1}{I\lambda_d}\sum_{\substack{f=1\\f\neq d}}^{2NM}\sum_{\substack{i=1\\i\neq d}}^{2NM}v_{f,d}v_{i,d}^*\mathbf{u}_f\mathbf{u}_i^H\\
-\ &\frac{1}{2I\sqrt{I}\lambda_d}[\sum_{\substack{f=1\\f\neq d}}^{2NM}\sum_{\substack{i=1\\i\neq d}}^{2NM}|v_{f,d}|^2v_{i,d}\mathbf{u}_i\mathbf{u}_d^H\\
+\ &\sum_{\substack{f=1\\f\neq d}}^{2NM}\sum_{\substack{i=1\\i\neq d}}^{2NM}v_{f,d}|v_{i,d}|^2\mathbf{u}_f\mathbf{u}_d^H + \sum_{\substack{f=1\\f\neq d}}^{2NM}\sum_{\substack{i=1\\i\neq d}}^{2NM}|v_{f,d}|^2v_{i,d}^*\mathbf{u}_d\mathbf{u}_i^H\\
+\ &\sum_{\substack{f=1\\f\neq d}}^{2NM}\sum_{\substack{i=1\\i\neq d}}^{2NM}|v_{i,d}|^2v_{f,d}^*\mathbf{u}_d\mathbf{u}_f^H] + O(\frac{1}{I^2})
\end{aligned}$$

and

$$\begin{aligned}
&\hat{\mathbf{u}}_d\frac{\beta_{d,d}}{\sqrt{I}\lambda_d^2}\hat{\mathbf{u}}_d^H \qquad (28)\\
=\ &[\frac{\beta_{d,d}}{\sqrt{I}\lambda_d^2}\mathbf{u}_d\mathbf{u}_d^H - \frac{\beta_{d,d}}{I\sqrt{I}\lambda_d^2}\sum_{\substack{f=1\\f\neq d}}^{2NM}|v_{f,d}|^2\mathbf{u}_d\mathbf{u}_d^H\\
+\ &\frac{\beta_{d,d}}{I\lambda_d^2}[\sum_{\substack{f=1\\f\neq d}}^{2NM}v_{f,d}\mathbf{u}_f\mathbf{u}_d^H + v_{f,d}^*\mathbf{u}_d\mathbf{u}_f^H]\\
+\ &\frac{\beta_{d,d}}{I\sqrt{I}\lambda_d^2}\sum_{\substack{f=1\\f\neq d}}^{2NM}\sum_{\substack{i=1\\i\neq d}}^{2NM}v_{f,d}v_{i,d}^*\mathbf{u}_f\mathbf{u}_i^H + O(\frac{1}{I^2})
\end{aligned}$$

Using (27) and (28), the mean of $\hat{\mathbf{u}}_d\hat{\lambda}_d^{-1}\hat{\mathbf{u}}_d^H$ is derived as

$$\begin{aligned}
&E\{\hat{\mathbf{u}}_d\hat{\lambda}_d^{-1}\hat{\mathbf{u}}_d^H\} \qquad (29)\\
=\ &\frac{1}{\lambda_d}\mathbf{u}_d\mathbf{u}_d^H - \frac{1}{I\lambda_d}\sum_{\substack{f=1\\f\neq d}}^{2NM}|v_{f,d}|^2\mathbf{u}_d\mathbf{u}_d^H\\
+\ &\frac{1}{I\lambda_d}\sum_{\substack{f=1\\f\neq d}}^{2NM}\sum_{\substack{i=1\\i\neq d}}^{2NM}v_{f,d}v_{i,d}^*\mathbf{u}_f\mathbf{u}_i^H + O(\frac{1}{I^2})\\
=\ &\frac{1}{\lambda_d}\mathbf{u}_d\mathbf{u}_d^H - \frac{1}{I\lambda_d}\sum_{\substack{f=1\\f\neq d}}^{2NM}|v_{f,d}|^2\mathbf{u}_d\mathbf{u}_d^H\\
+\ &\frac{1}{I\lambda_d}\sum_{\substack{f=1\\f\neq d}}^{2NM}\frac{\lambda_f\lambda_d}{(\lambda_d-\lambda_f)^2}\mathbf{u}_f\mathbf{u}_f^H + O(\frac{1}{I^2})
\end{aligned}$$

Appendix B

In this appendix, the performance of $E\{\mathbf{w}_{EV-t}^H\hat{\mathbf{h}}_1\}$ is analyzed for uncorrelated multipath propagation. Below the maximum peak corresponding to first path of first user is investigated. In this case, $E\{\mathbf{w}_{EV-t}^H\hat{\mathbf{h}}_1\}$ can be split into three parts according to the partition of $\hat{\mathbf{h}}_1$.

$$\begin{aligned}
E\{\mathbf{w}_{EV-t}^H\hat{\mathbf{h}}_1\}_{un} &= \check{\mathbf{h}}_1^H\sum_{d=1}^{D}E\{\hat{\mathbf{u}}_d\hat{\lambda}_d^{-1}\hat{\mathbf{u}}_d^H\}\hat{\mathbf{h}}_1 \qquad (30)\\
&= \underbrace{a_{1,1}\mathbf{h}_{1,1}^H\sum_{d=1}^{D}E\{\hat{\mathbf{u}}_d\hat{\lambda}_d^{-1}\hat{\mathbf{u}}_d^H\}\hat{\mathbf{h}}_1}_{A}\\
&\quad + \underbrace{\sum_{l=2}^{L}a_{1,l}\mathbf{h}_{1,l}^H\sum_{d=1}^{D}E\{\hat{\mathbf{u}}_d\hat{\lambda}_d^{-1}\hat{\mathbf{u}}_d^H\}\hat{\mathbf{h}}_1}_{B}
\end{aligned}$$

$$+ \quad \underbrace{\check{\mathbf{n}}\sum_{d=1}^{D} E\{\hat{\mathbf{u}}_d\hat{\lambda}_d^{-1}\hat{\mathbf{u}}_d^H\}\hat{\mathbf{h}}_1}_{C}$$

The A, B, and C parts correspond to the contribution of first path of first user, multipath interferences from first user, and noise interference respectively.

Performance analysis of part A

$$\begin{aligned} & a_{1,1}\mathbf{h}_{1,1}^H\sum_{d=1}^{D} E\{\hat{\mathbf{u}}_d\hat{\lambda}_d^{-1}\hat{\mathbf{u}}_d^H\}\hat{\mathbf{h}}_1 \qquad (31)\\ = \;& a_{1,1}\mathbf{h}_{1,1}^H\mathbf{u}_1\lambda_1^{-1}\mathbf{u}_1^H\hat{\mathbf{h}}_1 + \underbrace{a_{1,1}\sum_{d=2}^{D}\mathbf{h}_{1,1}^H\mathbf{u}_d\lambda_d^{-1}\mathbf{u}_d^H\hat{\mathbf{h}}_1}\\ - \;& a_{1,1}\frac{1}{I}\sum_{f=2}^{2NM}\frac{\lambda_f}{(\lambda_1-\lambda_f)^2}\mathbf{h}_{1,1}^H\mathbf{u}_1\mathbf{u}_1^H\hat{\mathbf{h}}_1\\ - \;& \underbrace{a_{1,1}\frac{1}{I}\sum_{d=2}^{D}\sum_{\frac{f=1}{f\neq d}}^{2NM}\frac{\lambda_f}{(\lambda_d-\lambda_f)^2}\mathbf{h}_{1,1}^H\mathbf{u}_d\mathbf{u}_d^H\hat{\mathbf{h}}_1}\\ + \;& \underbrace{a_{1,1}\frac{1}{I}\sum_{f=2}^{2NM}\frac{\lambda_f}{(\lambda_1-\lambda_f)^2}\mathbf{h}_{1,1}^H\mathbf{u}_f\mathbf{u}_f^H\hat{\mathbf{h}}_1}\\ + \;& a_{1,1}\frac{1}{I}\sum_{d=2}^{D}\sum_{\frac{f=1}{f\neq d}}^{2NM}\frac{\lambda_f}{(\lambda_d-\lambda_f)^2}\mathbf{h}_{1,1}^H\mathbf{u}_f\mathbf{u}_f^H\hat{\mathbf{h}}_1 + O(\frac{1}{I^2}) \end{aligned}$$

In 2×2 signal subspace, $\mathbf{h}_{1,1}^H\mathbf{u}_d\mathbf{u}_d^H\hat{\mathbf{h}}_1 = 0$ for $d\neq 1$ [22]. Through two-dimensional spectrum searching, (31) can be simplified as

$$\begin{aligned} & a_{1,1}\mathbf{h}_{1,1}^H\sum_{d=1}^{D}\hat{\mathbf{u}}_d\hat{\lambda}_d^{-1}\hat{\mathbf{u}}_d^H\hat{\mathbf{h}}_{1,1} \qquad (32)\\ = \;& a_{1,1}\mathbf{h}_{1,1}^H\mathbf{u}_1\lambda_1^{-1}\mathbf{u}_1^H\hat{\mathbf{h}}_{1,1} + \frac{1}{I}a_{1,1}\mathbf{h}_{1,1}^H\sum_{f=2}^{D}\frac{1}{\lambda_1-\lambda_f}\mathbf{u}_1\mathbf{u}_1^H\hat{\mathbf{h}}_{1,1}\\ - \;& \frac{1}{I}a_{1,1}\mathbf{h}_{1,1}^H\frac{\sigma^2(2NM-D)}{(\lambda_1-\sigma^2)^2}\mathbf{u}_1\mathbf{u}_1^H\hat{\mathbf{h}}_{1,1} + O(\frac{1}{I^2})\\ = \;& a_{1,1}\mathbf{h}_{1,1}^H\mathbf{u}_1\lambda_1^{-1}\mathbf{u}_1^H\hat{\mathbf{h}}_{1,1} + \chi a_{1,1}\mathbf{h}_{1,1}^H\mathbf{u}_1\mathbf{u}_1^H\hat{\mathbf{h}}_{1,1} + O(\frac{1}{I^2}) \end{aligned}$$

Performance analysis of part B

$$\begin{aligned} & \sum_{l=2}^{L}a_{1,l}\mathbf{h}_{1,l}^H\sum_{d=1}^{D}E\{\hat{\mathbf{u}}_d\hat{\lambda}_d^{-1}\hat{\mathbf{u}}_d^H\}\hat{\mathbf{h}}_1 \qquad (33)\\ = \;& \sum_{l=2}^{L}a_{1,l}\mathbf{h}_{1,l}^H\mathbf{u}_l{\lambda_l}^{-1}\mathbf{u}_l^H\hat{\mathbf{h}}_1 + \underbrace{\sum_{l=2}^{L}a_{1,l}\sum_{\frac{d=1}{d\neq l}}^{D}\mathbf{h}_{1,l}^H\mathbf{u}_d{\lambda_d}^{-1}\mathbf{u}_d^H\hat{\mathbf{h}}_1}\\ - \;& \frac{1}{I}\sum_{l=2}^{L}a_{1,l}\sum_{\frac{f=1}{f\neq l}}^{2NM}\frac{\lambda_f}{(\lambda_l-\lambda_f)^2}\mathbf{h}_{1,l}^H\mathbf{u}_l\mathbf{u}_l^H\hat{\mathbf{h}}_1\\ - \;& \underbrace{\frac{1}{I}\sum_{l=2}^{L}a_{1,l}\sum_{\frac{d=1}{d\neq l}}^{D}\sum_{\frac{f=1}{f\neq d}}^{2NM}\frac{\lambda_f}{(\lambda_d-\lambda_f)^2}\mathbf{h}_{1,l}^H\mathbf{u}_d\mathbf{u}_d^H\hat{\mathbf{h}}_1}\\ + \;& \underbrace{\frac{1}{I}\sum_{l=2}^{L}a_{1,l}\sum_{\frac{f=1}{f\neq l}}^{2NM}\frac{\lambda_f}{(\lambda_l-\lambda_f)^2}\mathbf{h}_{1,l}^H\mathbf{u}_f\mathbf{u}_f^H\hat{\mathbf{h}}_1}\\ + \;& \frac{1}{I}\sum_{l=2}^{L}a_{1,l}\sum_{\frac{d=1}{d\neq l}}^{D}\sum_{\frac{f=1}{f\neq d}}^{2NM}\frac{\lambda_f}{(\lambda_d-\lambda_f)^2}\mathbf{h}_{1,l}^H\mathbf{u}_f\mathbf{u}_f^H\hat{\mathbf{h}}_1\\ + \;& O(\frac{1}{I^2}) \end{aligned}$$

Because $\mathbf{h}_{1,l}^H\mathbf{u}_d\mathbf{u}_d^H\hat{\mathbf{h}}_1 = 0$ for $d\neq l$, the parts with underline are zeros. Meanwhile, as the searching point $\hat{\mathbf{h}}_1$ is on $\mathbf{h}_{1,1}$, $\mathbf{h}_{1,l}^H\mathbf{u}_l\mathbf{u}_l^H\hat{\mathbf{h}}_1 = 0$. Hence we get $\sum_{l=2}^{L}a_{1,l}\mathbf{h}_{1,l}^H\sum_{d=1}^{D}E\{\hat{\mathbf{u}}_d\hat{\lambda}_d^{-1}\hat{\mathbf{u}}_d^H\}\hat{\mathbf{h}}_1 = O(\frac{1}{I^2})$.

Performance analysis of part C. Because the vector $\check{\mathbf{n}}$ is linear independent with space-time response vectors, pre-multiplying and post-multiplying (41) by $\check{\mathbf{n}}^H$ and $\mathbf{u}_d$, $d = 1,...,D$, and using the orthogonality of eigenvectors, we get

$$\mathbf{0} = \lambda_d\check{\mathbf{n}}^H\mathbf{u}_d \qquad (34)$$

Post-multiplying (34) by $\mathbf{u}_d^H\hat{\mathbf{h}}_1$, we have

$$\check{\mathbf{n}}^H\mathbf{u}_d\mathbf{u}_d^H\hat{\mathbf{h}}_1 = \mathbf{0} \qquad (35)$$

Hence $\check{\mathbf{n}}\sum_{d=1}^{D}E\{\hat{\mathbf{u}}_d\hat{\lambda}_d^{-1}\hat{\mathbf{u}}_d^H\}\hat{\mathbf{h}}_1$ equals zero.

Finally the performance of (30) is derived as

$$\begin{aligned} & E\{\mathbf{w}_{EV-t}^H\hat{\mathbf{h}}_1\}_{un} \qquad (36)\\ = \;& a_{1,1}\mathbf{h}_{1,1}^H\mathbf{u}_1\lambda_1^{-1}\mathbf{u}_1^H\hat{\mathbf{h}}_{1,1} + \chi a_{1,1}\mathbf{h}_{1,1}^H\mathbf{u}_1\mathbf{u}_1^H\hat{\mathbf{h}}_1\\ + \;& O(\frac{1}{I^2}) \end{aligned}$$

APPENDIX C

The performance of $E\{\mathbf{w}_{EV-t}^H\hat{\mathbf{h}}_1\}$ in this appendix is evaluated in coherent multipath transmission. Same as Appendix B the performance of 1th user $1th$ path is investigated. We split $E\{\mathbf{w}_{EV-t}^H\hat{\mathbf{h}}_1\}_{co}$ into three parts according to the partition of $\check{\mathbf{h}}_1$. Then we get

$$\begin{aligned} E\{\mathbf{w}_{EV-t}^H\hat{\mathbf{h}}_1\}_{co} &= \check{\mathbf{h}}_1^H\sum_{d=1}^{D}E\{\hat{\mathbf{u}}_d\hat{\lambda}_d^{-1}\hat{\mathbf{u}}_d^H\}\hat{\mathbf{h}}_1 \qquad (37)\\ &= \underbrace{a_{1,1}\mathbf{h}_{1,1}^H\sum_{d=1}^{D}E\{\hat{\mathbf{u}}_d\hat{\lambda}_d^{-1}\hat{\mathbf{u}}_d^H\}\hat{\mathbf{h}}_1}_{A}\\ &+ \underbrace{\sum_{l=1}^{L}a_{1,l}\mathbf{h}_{1,l}^H\sum_{d=1}^{D}E\{\hat{\mathbf{u}}_d\hat{\lambda}_d^{-1}\hat{\mathbf{u}}_d^H\}\hat{\mathbf{h}}_1}_{B}\\ &+ \underbrace{\check{\mathbf{n}}\sum_{d=1}^{D}E\{\hat{\mathbf{u}}_d\hat{\lambda}_d^{-1}\hat{\mathbf{u}}_d^H\}\hat{\mathbf{h}}_1}_{C} \end{aligned}$$

The A, B, and C parts are the contribution from first path of first path, multipath interferences from first user, and noise interference respectively.

Performance analysis of part A

$$
\begin{aligned}
& a_{1,1}\mathbf{h}_{1,1}^H \sum_{d=1}^{D} E\{\hat{\mathbf{u}}_d \hat{\lambda}_d^{-1} \hat{\mathbf{u}}_d^H\} \hat{\mathbf{h}}_1 \qquad (38)\\
= \;& a_{1,1}\mathbf{h}_{1,1}^H \mathbf{u}_1 \lambda_1^{-1} \mathbf{u}_1^H \hat{\mathbf{h}}_1 + \underbrace{a_{1,1} \sum_{d=2}^{D} \mathbf{h}_{1,1}^H \mathbf{u}_d \lambda_d^{-1} \mathbf{u}_d^H \hat{\mathbf{h}}_1}\\
- \;& a_{1,1} \frac{1}{I} \sum_{f=2}^{2NM} \frac{\lambda_f}{(\lambda_1 - \lambda_f)^2} \mathbf{h}_{1,1}^H \mathbf{u}_1 \mathbf{u}_1^H \hat{\mathbf{h}}_1\\
- \;& \underbrace{a_{1,1} \frac{1}{I} \sum_{d=2}^{D} \sum_{\substack{f=1 \\ f \neq d}}^{2NM} \frac{\lambda_f}{(\lambda_d - \lambda_f)^2} \mathbf{h}_{1,1}^H \mathbf{u}_d \mathbf{u}_d^H \hat{\mathbf{h}}_1}\\
+ \;& \underbrace{a_{1,1} \frac{1}{I} \sum_{f=2}^{2NM} \frac{\lambda_f}{(\lambda_1 - \lambda_f)^2} \mathbf{h}_{1,1}^H \mathbf{u}_f \mathbf{u}_f^H \hat{\mathbf{h}}_1}\\
+ \;& a_{1,1} \frac{1}{I} \sum_{d=2}^{D} \sum_{\substack{f=1 \\ f \neq d}}^{2NM} \frac{\lambda_f}{(\lambda_d - \lambda_f)^2 \mathbf{h}_{1,1}^H} \mathbf{u}_f \mathbf{u}_f^H \hat{\mathbf{h}}_1 + O(\frac{1}{I^2})\\
= \;& a_{1,1}\mathbf{h}_{1,1}^H \mathbf{u}_1 \lambda_1^{-1} \mathbf{u}_1^H \hat{\mathbf{h}}_1 + \frac{1}{I} a_{1,1} \sum_{f=2}^{D} \frac{1}{\lambda_1 - \lambda_f} \mathbf{h}_{1,1}^H \mathbf{u}_1 \mathbf{u}_1^H \hat{\mathbf{h}}_1\\
- \;& \frac{1}{I} a_{1,1} \frac{\sigma^2 (2NM - D)}{(\lambda_1 - \sigma^2)^2} \mathbf{h}_{1,1}^H \mathbf{u}_1 \mathbf{u}_1^H \hat{\mathbf{h}}_1 + O(\frac{1}{I^2})\\
= \;& a_{1,1}\mathbf{h}_{1,1}^H \mathbf{u}_1 \lambda_1^{-1} \mathbf{u}_1^H \hat{\mathbf{h}}_1 + \chi a_{1,1} \mathbf{h}_{1,1}^H \mathbf{u}_1 \mathbf{u}_1^H \hat{\mathbf{h}}_1 + O(\frac{1}{I^2})
\end{aligned}
$$

In above function $\mathbf{h}_{1,1}^H \mathbf{u}_d \mathbf{u}_d^H \hat{\mathbf{h}}_1 = 0$ for $d \neq 1$.

Performance analysis of part B Part B of (37) can be decomposed and derived as

$$
\begin{aligned}
& \sum_{l=1}^{L} a_{1,l} \mathbf{h}_{1,l}^H \sum_{d=1}^{D} E\{\hat{\mathbf{u}}_d \hat{\lambda}_d^{-1} \hat{\mathbf{u}}_d^H\} \hat{\mathbf{h}}_1 \qquad (39)\\
= \;& \sum_{l=2}^{L} a_{1,l} \mathbf{h}_{1,l}^H \mathbf{u}_1 \lambda_1^{-1} \mathbf{u}_1^H \hat{\mathbf{h}}_1 + \underbrace{\sum_{l=2}^{L} a_{1,l} \sum_{d=2}^{D} \mathbf{h}_{1,l}^H \mathbf{u}_d \lambda_d^{-1} \mathbf{u}_d^H \hat{\mathbf{h}}_1}\\
- \;& \frac{1}{I} \sum_{l=2}^{L} a_{1,l} \sum_{f=2}^{2NM} \frac{\lambda_f}{(\lambda_1 - \lambda_f)^2} \mathbf{h}_{1,l}^H \mathbf{u}_1 \mathbf{u}_1^H \hat{\mathbf{h}}_1\\
- \;& \underbrace{\frac{1}{I} \sum_{l=2}^{L} a_{1,l} \sum_{d=2}^{D} \sum_{\substack{f=1 \\ f \neq d}}^{2NM} \frac{\lambda_f}{(\lambda_d - \lambda_f)^2} \mathbf{h}_{1,l}^H \mathbf{u}_d \mathbf{u}_d^H \hat{\mathbf{h}}_1}\\
+ \;& \underbrace{\frac{1}{I} \sum_{l=2}^{L} a_{1,l} \sum_{f=2}^{2NM} \frac{\lambda_f}{(\lambda_1 - \lambda_f)^2} \mathbf{h}_{1,l}^H \mathbf{u}_f \mathbf{u}_f^H \hat{\mathbf{h}}_1}\\
+ \;& \frac{1}{I} \sum_{l=2}^{L} a_{1,l} \sum_{d=2}^{D} \sum_{\substack{f=1 \\ f \neq d}}^{2NM} \frac{\lambda_f}{(\lambda_d - \lambda_f)^2} \mathbf{h}_{1,l}^H \mathbf{u}_f \mathbf{u}_f^H \hat{\mathbf{h}}_1 + O(\frac{1}{I^2})\\
= \;& \sum_{l=2}^{L} a_{1,l} \mathbf{h}_{1,l}^H \mathbf{u}_1 \lambda_1^{-1} \mathbf{u}_1^H \hat{\mathbf{h}}_1\\
+ \;& \frac{1}{I} \sum_{l=2}^{L} a_{1,l} \mathbf{h}_{1,l}^H \sum_{d=2}^{D} \frac{1}{\lambda_1 - \lambda_d} \mathbf{u}_1 \mathbf{u}_1^H \hat{\mathbf{h}}_1\\
- \;& \frac{1}{I} \sum_{l=2}^{L} a_{1,l} \mathbf{h}_{1,l}^H \frac{(2NM - D)\sigma^2}{(\lambda_1 - \sigma^2)^2} \mathbf{u}_1 \mathbf{u}_1^H \hat{\mathbf{h}}_1 + O(\frac{1}{I^2})\\
= \;& \sum_{l=2}^{L} (a_{1,l} \lambda_1^{-1} + \chi a_{1,l}) \mathbf{h}_{1,l}^H \mathbf{u}_1 \mathbf{u}_1^H \hat{\mathbf{h}}_1 + O(\frac{1}{I^2})
\end{aligned}
$$

In (39), $\mathbf{h}_{1,l}^H \mathbf{u}_d \mathbf{u}_d^H \hat{\mathbf{h}}_1 = 0$ for $d \neq 1$.

Performance analysis of part C Because $\check{\mathbf{n}}^H \mathbf{u}_d \mathbf{u}_d^H \hat{\mathbf{h}}_1 = \mathbf{0}$, we get $\check{\mathbf{n}} \sum_{d=1}^{D} E\{\hat{\mathbf{u}}_d \hat{\lambda}_d^{-1} \hat{\mathbf{u}}_d^H\} \hat{\mathbf{h}}_1 = \mathbf{0}$.

At last, the performance of $E\{\mathbf{w}_{EV-t}^H \hat{\mathbf{h}}_{1,1}\}_{co}$ is derived as

$$
\begin{aligned}
& E\{\mathbf{w}_{EV-t}^H \hat{\mathbf{h}}_{1,1}(\theta, \tau)\}_{co} \qquad (40)\\
= \;& a_{1,1}\mathbf{h}_{1,1}^H \mathbf{u}_1 \lambda_1^{-1} \mathbf{u}_1^H \hat{\mathbf{h}}_1 + \chi a_{1,1} \mathbf{h}_{1,1}^H \mathbf{u}_1 \mathbf{u}_1^H \hat{\mathbf{h}}_1\\
+ \;& \sum_{l=2}^{L} (a_{1,l} \lambda_1^{-1} + \chi a_{1,l}) \mathbf{h}_{1,l}^H \mathbf{u}_1 \mathbf{u}_1^H \hat{\mathbf{h}}_1 + O(\frac{1}{I^2})
\end{aligned}
$$

APPENDIX D

Let $\mathbf{H}\mathbf{R}_F(i)\mathbf{H}^H$ denote the noise free correlation matrix. It can be eigen-decomposed as

$$\mathbf{H}\mathbf{R}_F(i)\mathbf{H}^H = \sum_{d=1}^{D} \dot{\lambda}_d \mathbf{u}_d \mathbf{u}_d^H \qquad (41)$$

$\dot{\lambda}_d$, $d = 1, \cdots, D$, are noise free eigenvalues. $\dot{\lambda}_d$ is related to λ_d by $\dot{\lambda}_d = \lambda_d - \sigma^2$.

Because space-time response vectors in $\mathbf{H}$ are orthogonal, we get

$$
\begin{aligned}
& \sum_{d=1}^{D} \dot{\lambda}_d = tr\{\mathbf{H}\mathbf{R}_F(i)\mathbf{H}^H\} \qquad (42)\\
= \;& E\{|a_{1,1,i}|^2\} \sum_{k=1}^{K} \sum_{l=1}^{L}\\
& (\underline{|\mathbf{h}|}_{k,l}^2 |\beta|_{k,l,i-1}^2 + |\mathbf{h}|_{k,l}^2 |\beta|_{k,l,i}^2 + \overline{|\mathbf{h}|}_{k,l}^2 |\beta|_{k,l,i+1}^2)
\end{aligned}
$$

where $|\beta|_{k,l,i-1}^2 = \frac{E\{|a_{k,l,i-1}|^2\}}{E\{|a_{1,1,i}|^2\}}$, $|\beta|_{k,l,i}^2 = \frac{E\{|a_{k,l,i}|^2\}}{E\{|a_{1,1,i}|^2\}}$, and $|\beta|_{k,l,i+1}^2 = \frac{E\{|a_{k,l,i+1}|^2\}}{E\{|a_{1,1,i}|^2\}}$. $\overline{|\mathbf{h}|}_{k,l}^2 = M\tau_{k,l}$, $|\mathbf{h}|_{k,l}^2 = MN$, and $\underline{|\mathbf{h}|}_{k,l}^2 = M(N - \tau_{k,l})$ (see Appendix E). (42) shows that $\dot{\lambda}_d$, $d = 1, \cdots, D$, are proportional with signal strengths and the number of antenna elements. If σ^2 is small enough, $\lambda_d \approx \dot{\lambda}_d$. Therefore we can suppose λ_d, $d = 1, \cdots, D$, are proportional with the signal strengths and the number of antenna elements.

APPENDIX E

The correlation functions of code vectors are

$$
\begin{aligned}
\underline{|\mathbf{c}|}_{k,l}^2 &= \underline{\mathbf{c}}_{k,l}^T \underline{\mathbf{c}}_{k,l} = \tau_{k,l} && (43)\\
|\mathbf{c}|_{k,l}^2 &= \mathbf{c}_{k,l}^T \mathbf{c}_{k,l} = N && (44)\\
\overline{|\mathbf{c}|}_{k,l}^2 &= \overline{\mathbf{c}}_{k,l}^T \overline{\mathbf{c}}_{k,l} = N - \tau_{k,l} && (45)
\end{aligned}
$$

Hence, the correlation functions of space-time response vectors are derived as

$$\underline{|\mathbf{h}|}^2_{k,l} = \underline{\mathbf{h}}^H_{k,l}\underline{\mathbf{h}}_{k,l} = M\tau_{k,l} \quad (46)$$

$$|\mathbf{h}|^2_{k,l} = \mathbf{h}^H_{k,l}\mathbf{h}_{k,l} = MN \quad (47)$$

$$\overline{|\mathbf{h}|}^2_{k,l} = \overline{\mathbf{h}}^H_{k,l}\overline{\mathbf{h}}_{k,l} = M(N-\tau_{k,l}) \quad (48)$$

REFERENCES

[1] M.D. Katz, J.H.J. Iinatti, S. Glisic, "Two-dimensional code acquisition in time and angle domains", IEEE Journal on Selected Areas Communication, vol. 19, pp. 2441-2451, Dec. 2001.
[2] M. Wax, A. Leshem, "Joint estimation of time delays and directions of arrival of multiple reflections of a known signal", IEEE Trans. on Signal Processing, vol. 45, pp. 2477-2484, Oct. 1997.
[3] K. Wang, H. Ge, Joint Space-Time Channel Parameter Estimation for DS-CDMA System in Multipath Rayleigh Fading Channels, Electronics Letters, vol. 37, pp. 458-460, Mar. 2001
[4] Y.Y. Wang, J.T. Chen; W.H. Fang, "TST-MUSIC for joint DOA-delay estimation", IEEE Trans. on Signal Processing," vol. 49, pp. 721 -729, Apr. 2001
[5] Z. Gu, E. Gunawan, "Joint space-time estimation for DS-CDMA system in fast fading multipath channel", IEEE Electronics Letters, vol. 37, pp. 1407 -1408, Nov. 2001.
[6] M.C. Vanderveen, C.B. Papadias, A. Paulraj, "Joint angle and delay estimation (JADE) for multipath signals arriving at an antenna array", IEEE Communications Letters, vol. 1, pp. 12 -14, Jan. 1997.
[7] M.C. Vanderveen, A.-J. Van der Veen, and A. Paulraj, "Estimation of Multipath Parameters in Wireless Communications", IEEE Trans. on Signal Processing, vol. 46, pp. 682-690, Mar, 1998
[8] A.-J. Van der Veen, M.C. Vanderveen, A. Paulraj, "Joint angle and delay estimation using shift-invariance properties", IEEE Signal Processing Letters, vol. 4, pp. 142 -145, May 1997.
[9] A.-J. Van der Veen, M.C. Vanderveen, A. Paulraj, "Joint angle and delay estimation using shift-invariance techniques", IEEE Trans. on Signal Processing, vol. 46, pp. 405-418, Feb. 1998.
[10] R.O. Schmidt, "Multiple emitter location and signal parameter estimation", IEEE Trans. Antennas and Propagation, vol. 43, pp. 276-280, Mar. 1986.
[11] R. Roy, T. Kailath, "ESPRIT–Estimation of signal parameters via rational invariance techniques", IEEE trans. Acoust., Speech, Signal Processing, vol. 37, pp. 984-995, Jul. 1989.
[12] R. Kumaresan, D.W. Tufts, "estimating the angles of arrival of multiple plane waves", IEEE Trans. Aerosp. Electron. Syst., vol. AES-19, pp.134-139, jan. 1983.
[13] P. Stoica, K.C. Sharman, "Novel eigenanalysis method for direction estimation", Proc. Inst. Elect. Eng. F, vol. 137, no. 1, pp. 19-26, 1990.
[14] M. Viberg, B. Ottersten, "Sensor array processing based on subspace fitting", IEEE Trans. on Signal processing, vol. 39, pp. 1110-1121, May 1991.
[15] M. Viberg, B. Ottersten, T. Kailath, "Detection and estimation in sensor arrays using weighted subspace fitting", IEEE. Trans. on Signal Processing, vol. 39, pp. 2436-2449, Nov. 1991
[16] B. Ottersten, M. Viberg, P. Stoica, A, Nehorai, "Exact and large sample maximum likelihood techniques for parameter estimation and detection in array processing", Radar Array Processing, chap. 4, pp.99-151, Springer-Verlag, Berlin, 1993
[17] D.H. Johnson, S. DeGraaf, "Improving the Resolution of Bearing in Passive Sonar Arrays by Eigenvalue Analysis", IEEE Trans. on Signal Processing, vol. ASSP-30, pp.638-647, Aug. 1982.
[18] T. Shen, M. Wax, T. Kailath, "On spatial smoothing of direction-of-arrival estimation of coherent signals", IEEE Trans. on Acoustics, Speech, and Signal Processing, vol. 33, pp. 806-811, Aug. 1985.
[19] S.U. Pillai, B.H. Kwon, "Forward/backward spatial smoothing techniques for coherent signal identification", IEEE Trans. on Acoustics, Speech, and Signal Processing, vol. 37, pp. 8-15, Jan. 1989.
[20] J. H. Wilkinson, The Algebraic Eigenvalue Problem. New York: Oxford University Press, 1965.
[21] S.U. Pillai, Array Signal Processing. New York: Springer-Verlag, 1989.
[22] L. Chang, C.C. Yeh, "Performance of DMI and Eigenspace-Based beamformers", IEEE Trans. on Signal Processing, vol. 40, pp. 1336-1347, Nov. 1992.